Search for ferromagnetism in SnO$_2$ doped with transition metals (V, Mn, Fe, and Co)

X L Wang, Z X Dai and Z Zeng[1]

Key Laboratory of Materials Physics, Institute of Solid State Physics, Chinese Academy of Sciences, Hefei 230031, People's Republic of China
and
Graduate School of the Chinese Academy of Sciences, People's Republic of China

E-mail: zzeng@theory.issp.ac.cn

Abstract

Based on first-principles calculations, we have investigated electronic structures and magnetic properties of SnO$_2$ doped with V, Mn, Fe, and Co. Our results show that ferromagnetism is the ground state and that the Curie temperatures are expected to have high values for Fe- and Co-doped SnO$_2$, which is in good agreement with the experimental observations (Ogale *et al* 2003 *Phys. Rev. Lett.* **91** 077205; Coey *et al* 2004 *Appl. Phys. Lett.* **84** 1332). However, in V- and Mn-doped SnO$_2$, paramagnetism is more stable than ferromagnetism. In addition, we also probe the effect of an oxygen vacancy. The results exhibit that an oxygen vacancy strongly influences the magnetic properties of these doped systems, and an oxygen vacancy strongly attracts Fe and Co ions. As a result, transition metal–oxygen vacancy–transition metal groups will be common in Fe- and Co-doped SnO$_2$, but this tendency does not exist in the cases of V and Mn doping. In V-doped SnO$_2$, ferromagnetism becomes more stable than antiferromagnetism after inducing additional n-type carriers and the Curie temperature increases with increasing density of n-type carriers. Hence, raising the density of n-type carriers is a practical way to realize high Curie temperatures in V-doped SnO$_2$.

1. Introduction

In recent years, oxide diluted magnetic semiconductors (ODMS) have attracted considerable attention both theoretically and experimentally because of their projected potential applications in spintronics devices. Especially after the observation of high temperature ferromagnetism (FM) in Co-doped anatase TiO$_2$ [3], many research groups have reported the room-temperature FM in various kinds of transition metal (TM) ion-doped ODMS, such as TM ion-doped ZnO [4–6], TiO$_2$ [7], and SnO$_2$ [1, 2, 8–10]. However, many controversial issues are still debated in this research field. For example, agreement on the origin of the ferromagnetic coupling has not yet been reached. Note that, the carrier-(hole-) mediated mechanism and double exchange mechanism, which are known to account for the FM in Mn-doped GaAs and mixed valence manganite respectively, may not account for the ferromagnetic behavior shown in ODMS. Some people believed that FM in ODMS might come from the presence of TM clusters;

Shinde *et al* [12], for example, claimed that the FM of their Co-doped TiO$_2$ thin films, which were deposited on R-Al$_2$O$_3$ substrate by pulsed-laser deposition, comes from Co nanoclusters. Nevertheless, there is clear evidence showing the absence of TM clusters [1, 5, 7]. Ramachandran *et al* [5] used pulsed-laser deposition to grow Co-doped ZnO films and claimed that the room-temperature FM of the films came from substituted, not second phase, Co^{2+}. Also, the properties of ODMS seem very sensitive to the experimental conditions: oxygen partial pressure, substrate temperature, and doping concentration [4, 7, 8], implying that micro-structures may influence the properties of these compounds strongly. In addition, oxygen vacancy (Vac(O)) may have a great influence on the properties of ODMS as Hong *et al* [8] showed that substrate size and oxygen partial pressure strongly influenced the properties of ODMS films which were fabricated by pulse-laser deposition. Coey *et al* [2] proposed an exchange mechanism that involves the Vac(O)s named F-center, and they expected that TM–Vac(O)–TM groups would be common in Fe-doped SnO$_2$. Another main controversial issue is that doping nonmagnetic

---

[1] Author to whom any correspondence should be addressed.

elements, such as V, can produce strongly ferromagnetic samples [8]. Sato and Katayama-Yoshida reported that V was the most promising dopant for ZnO in order to obtain a high Curie temperature theoretically [13]. V-doped TiO$_2$ and ZnO thin films were reported to have room-temperature Curie temperature [7, 20]. Among all the dopants, V was suggested to be the best candidate for doped TiO$_2$ experimentally [7], since a giant magnetic moment was observed. Saeki *et al* [20] observed room-temperature FM in V-doped ZnO films and only n-type metallic samples fabricated by lowering oxygen partial pressure were magnetic. They claimed that the magnetic properties of the films depended on the concentration of V ions and the density of carriers. However, we have not seen the report of the high Curie temperature for V-doped SnO$_2$ film.

Motivated by these controversial issues, many theoretical studies have been done in this field [14–19]. Spaldin [15] using the local spin-density approximation (LSDA), showed that FM did not exist in Co- and Mn-doped ZnO, unless additional p-type carriers were also incorporated. Recently, density-functional calculations of Co-doped TiO$_2$ with the generalized gradient approximation (GGA) were performed by Jaffe *et al* [18]. They reported that Vac(O)s played an important role in determining the magnetic properties of the compound and that Co ions tended to form complexes with Vac(O)s. However, theoretical work about TM ion-doped SnO$_2$ was lacking. Therefore, in the current work we investigate the electronic structures and magnetic properties of V- , Mn- , Fe- , and Co-doped SnO$_2$ over a range of concentrations by employing the first-principles methods. Our results show that FM is the ground state for Fe- and Co-doped SnO$_2$, and that paramagnetism is more stable than FM in V- and Mn-doped SnO$_2$. In doped SnO$_2$, Vac(O) has a strong influence on the magnetic properties of the doped compounds, and also has a strong tendency to be close to Fe and Co ions, but V ions exclude Vac(O) strongly. Mn ions only have a small influence on the distribution of Vac(O)s. Our results also exhibit that additional n-type carriers are required to stabilize the ferromagnetic state and that Curie temperature increases with the increase of the density of n-type carriers in V-doped SnO$_2$.

This paper is organized as follows: The computational method and theoretical model are briefly described in section 2, the results and discussions are presented in section 3, and a summary is given in section 4.

2. Computational details

All calculations have been performed in the framework of the density-functional theory (DFT) [21], which is implemented in the well-tested SIESTA code [22–24]. Only the valence electrons are considered in the calculations, and the core electrons are described by norm-conserving pseudopotentials constructed using the Troullier–Martins parameterization [25], including nonlinear core corrections [26] for TM ions and Sn. The adopted pseudopotentials have been proved to give good agreements with experiments as well as other *ab initio* calculations [15, 27–30], and we test them on the atomic scale. For the valence electrons, the wavefunctions are expanded by

the linear combination of atomic orbital (LCAO). In the current work, a double-ζ basis is used for Sn and O valence orbitals, showing that the discrepancy of the lattice parameter is within 2% for bulk SnO$_2$ in our test calculation. Since the d orbitals of TM ions are crucial to determine the magnetic properties of these diluted compounds, we use a triple-ζ basis for the d orbitals of TM ions. The radius cutoff for these functions is determined by an energy shift parameter of 0.02 Ryd. By using these orbital parameters the calculated properties converge to what is obtained by the greater basis and larger confinement radii within a reasonable precision criterion, for example, the changes of energy differences between ferromagnetic and antiferromagnetic states are less than 3 meV. As is well known, the ground state of bulk Fe is described better with GGA than that with LSDA. Therefore, the calculations about Fe-doped SnO$_2$ are performed with GGA and the functional of Perdew, Burke, and Ernzerhof known as PBE [31] is adopted. Other calculations are performed using LSDA and the Ceperley–Alder functional [32].

To simulate the doped compound, supercells ($2 \times 2 \times 2$) containing 48 atoms and the experimental lattice constant are used. One or two Sn atoms are substituted by TM ions to present 6.25% and 12.5% doping concentrations. We also probe the influence of oxygen vacancy Vac(O) on the TM ion-doped SnO$_2$ by inducing three kinds of Vac(O)s in our supercell calculations. The energy of 150 Ryd is used to define the finite real space grid for numerical integrals and the Brillouin zone is sampled by a $3 \times 3 \times 3$ Monkhorst and Pack grid [33]. The convergence criterion for the density matrix is 10^{-4}. Relaxation has been done in the case of V-doped SnO$_2$, the results show that, after relaxation, the distance between two V ions are shortened by less than 4%, hence, we do not discuss the structural relaxation of the atomic positions in this work.

3. Results and discussions

Based on the method mentioned above, we first calculate the electronic structure of rutile SnO$_2$ without doping TM ions. The calculated band gap of SnO$_2$ (1.1 eV) is smaller than the experimental value (3.6 eV), due to the well-known underestimation of the band gap by the DFT calculations with LDA, and the pure SnO$_2$ is a nonmagnetic one. These results are consistent with previous calculations [27].

3.1. TM ion-doped SnO$_2$

To investigate the electronic structure properties of TM ion-doped SnO$_2$, firstly, we substitute one Sn atom with one single TM ion in the supercell to simulate the doping concentration of 6.25%. When one TM ion is introduced in each supercell, the spin states of the doped compounds are forced to be ferromagnetic. The obtained DOS of TM ion (V, Mn, Fe, and Co)-doped SnO$_2$ are presented in figures 1(a)–(d), respectively. In TM ion-doped rutile SnO$_2$, O ions around TM ions form an octahedral crystal field, splitting d orbitals into lower t$_{2g}$ states and upper e$_g$ states as indicated in figure 1. The crystal field splitting between t$_{2g}$ and e$_g$ states is larger than the exchange splitting between t$_{2g}$ states in V- , Fe- , and Co-doped SnO$_2$, and these two terms almost have the same value
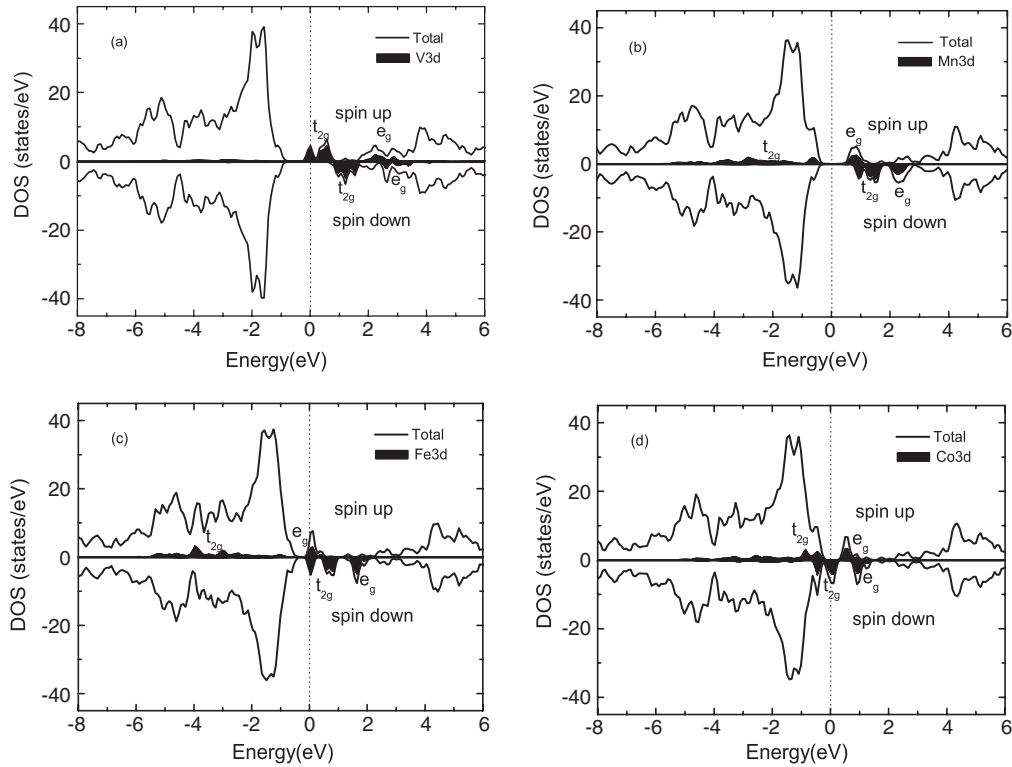
Figure 1. TM ion (V, Mn, Fe, and Co) 3d states (shaded) and total states (solid) of TM ion-doped SnO$_2$ in the case of 6.25% doping are shown in (a)–(d), respectively.

in Mn-doped SnO$_2$. As a result, low spin states of TM ions are expected in these compounds. The resulting magnetic moments for TM ions in V- , Mn- , Fe- , and Co-doped SnO$_2$ are 1.12 μ_B, 3.12 μ_B, 2.83 μ_B, and 0.78 μ_B respectively. This is similar to the case of TM ion-doped rutile TiO$_2$ carried out by Errico *et al* [19], where they obtained low spin states for Mn (2.52 μ_B), Fe (2.24 μ_B), and Co (0.63 μ_B) ions, whereas it is different from that of TM ion-doped ZnO. Applying first-principles calculations on Fe- and Co-doped ZnO [16], Park and Min have found that the exchange splitting is larger than the crystal field spitting in Fe- and Co-doped ZnO, and high magnetic moments are obtained for Fe (4.11 μ_B) and Co (2.92 μ_B) ions. The reason is that, in TM ion-doped SnO$_2$, TM ions have an octahedral coordination of ligands, but are placed in a tetrahedral coordination ligand field in TM ion-doped ZnO. The crystal field created by the octahedral coordination of ligand field is twice as large as that created by the tetrahedral coordination [34]. As shown in figures 1(a)–(d), the filled 3d states of Mn, Fe, and Co are strongly hybridized with the O 2p states, giving a broad band with a width comparable to O 2p states. Only V 3d states are mostly localized within the band-gap region and the filled V 3d states are higher in energy than other TM ion (Mn, Fe, and Co) counterparts. Since the hybridization implies the intensity of chemical reaction and strong hybridization brings about a big solubility, the above results mean that the substituent concentration of V-doped SnO$_2$ will be less than those of Mn, Fe, and Co-doped SnO$_2$. Among the four cases considered here, a metallic electronic structure is obtained only in Fe-doped SnO$_2$, for that the Fermi level crosses the sharp e$_g$

(spin up) and t$_{2g}$ (spin-down) states (figure 1(c)). While for V- and Co-doped SnO$_2$ shown in figures 1(a) and (d), they are half-metallic with the Fermi level crossing the sharp t$_{2g}$ states (spin up for V-doped and spin-down for Co-doped system). It is known that the narrow partially filled states near the Fermi level would have a metal–insulator transition driven by the Coulomb correlation interaction and/or the Jahn–Teller effect. However, the contributions to such a transition from e$_g$ and t$_{2g}$ are different due to the directional characteristics of e$_g$ and t$_{2g}$. Since t$_{2g}$ orbitals do not point to the octahedral apexes (oxygen positions) in an octahedral crystal field, the Jahn–Teller effect is weak and has a weak influence on the metal–insulator transition in V- and Co-doped SnO$_2$ systems with t$_{2g}$ contributions in comparison to the Fe-doped case with e$_g$ contributions in addition to the t$_{2g}$ contributions, as shown in figure 1. Our results exhibit that Mn-doped SnO$_2$ is a semiconductor shown in figure 1(b). Additionally, figures 1(c) and (d) also show that there are not only TM-d states but also the oxygen 2p states staying at the Fermi level, which are induced by TM ions, showing strong p–d coupling and hopping in Fe- and Co-doped SnO$_2$. However, as shown in figures 1(a) and (b), p–d coupling and hopping are weak in V- and Mn-doped cases.

In order to gain more insight into the properties of these TM ion-doped systems, we also investigate the two TM ion-doped SnO$_2$, corresponding to 12.5% doping concentration. Moreover, these two TM ion-doped SnO$_2$ compounds are probed via two different doped configurations. One is that the TM ions occupy the positions as far as possible and that they are connected via –O–Sn–O– bonds. The other is that TM ions
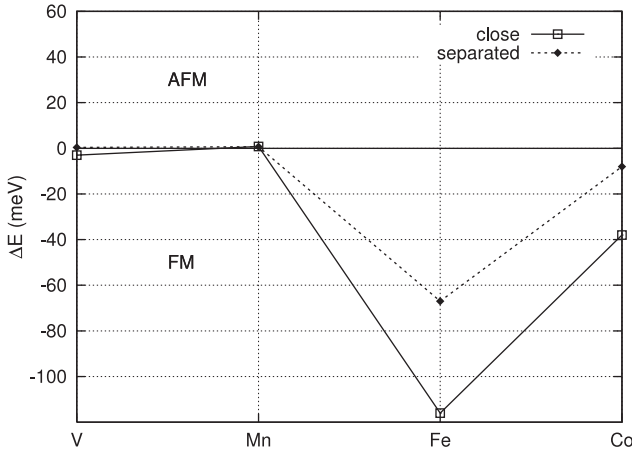
Figure 2. The energy difference ΔE between FM and AFM of TM ions (V, Mn, Fe, and Co)-doped SnO$_2$ in the case of 12.5% doping for the separated and close configurations.

Table 1. Magnetic moments (in μ_{B}) of the TM1 (μ^{TM1}) and TM2 (μ^{TM2}) in the separated and close configurations in the case of 12.5% doping concentration.

System	V-doped SnO$_2$ $\mu^{\mathrm{TM1}}/\mu^{\mathrm{TM2}}$	Mn-doped SnO$_2$ $\mu^{\mathrm{TM1}}/\mu^{\mathrm{TM2}}$	Fe-doped SnO$_2$ $\mu^{\mathrm{TM1}}/\mu^{\mathrm{TM2}}$	Co-doped SnO$_2$ $\mu^{\mathrm{TM1}}/\mu^{\mathrm{TM2}}$
Separated	1.17/1.17	3.12/3.12	3.58/3.58	0.79/0.79
Close	1.17/1.18	3.12/3.13	3.58/3.51	0.73/0.81

are only separated by one single O ion. We refer to these two cases as the separated and close configurations, respectively. In order to realize these configurations, one TM ion named TM1 is fixed in the origin of the supercell, and the other TM ion named TM2 moves along the (111) direction. We calculate the total energy in the ferromagnetic state (E_{fm}) as well as in the spin anti-ferromagnetic state (E_{afm}) for both configurations. Note that the non-collinear magnetic states are not considered in our work, due to the restrictions of the theoretical method. The energy difference ΔE between E_{fm} and E_{afm} is defined as follows:

$$\Delta E = E_{\mathrm{fm}} - E_{\mathrm{afm}}. \qquad (1)$$

The obtained energy differences ΔE for both configurations are shown in figure 2. For these doped systems, negative ΔE value means that FM is the ground state, and positive ΔE value means that AFM is the ground state. If ΔE is nearly zero, it means that paramagnetism is the ground state for the doped compound. As observed from this figure, in the cases of V- and Mn-doped SnO$_2$, ΔE is small for both separated and close configurations and then paramagnetism is the ground state without additional carriers or impurities. However, FM is more stable than AFM in Fe- and Co-doped SnO$_2$. The large absolute values of ΔE indicate that the Curie temperatures are expected to be high in Fe- and Co-doped SnO$_2$, if we approximately take 1 meV $\sim$ 10 K. This gives the same indication as the experimental observations: Ogale *et al* [1] reported that their films of Co-doped SnO$_2$ grown on *R*-plane sapphire by pulsed-laser deposition exhibited FM with a Curie temperature close to 650 K. Coey *et al* [2] also used pulsed-laser deposition to grow the Fe-doped SnO$_2$ thin films, in which the Curie temperature of 610 K was obtained. Also Punnose *et al* [9] synthesized powder samples of Fe-doped SnO$_2$, where the ferromagnetic samples displayed a Curie temperature $T_{\mathrm{C}} = 850$ K. Both for Fe- and Co-doped SnO$_2$, the absolute values of ΔE rapidly increase when TM ions move close to each other. Note that our calculations show that the close configuration is energetically more favorable than the separated one by around 95 meV, 75 meV, 17 meV, and

2 meV for Co-, Fe-, V-, and Mn-doped SnO$_2$, respectively, implying that Co and Fe ions have a strong tendency to cluster together during growth so that TM clusters are easily formed in Co- and Fe-doped SnO$_2$. On the contrary, the tendency to form a cluster is drastically reduced for the Mn- and V-doped cases. In contrast to Co and Fe, Mn and V might distribute themselves evenly throughout the lattice.

Recently, Janisch *et al* [11] pointed out that the 90° superexchange mechanism indeed leads to ferromagnetic coupling between the magnetic moments of neighboring Co ions in the Co-doped TiO$_2$ anatase, which has the situation of a 102° TM–anion–TM bond. Since the 90° TM–anion–TM bond also exists in rutile SnO$_2$, they indicated that rutile SnO$_2$ is a promising candidate for high temperature ferromagnets. In the close configuration chosen in our calculations, the TM–anion–TM bond angle is about 129°, hence the 90° superexchange works and will play an important effect in determining the ground state of the doped system. Considering our calculated electronic structures of TM ion-doped SnO$_2$ shown in figures 1(a)–(d), we attribute the ferromagnetism of Fe- and Co-doped SnO$_2$ to the 90° superexchange. Janisch *et al* [11] claimed that the cation d orbitals interact with their neighboring anion p orbitals via a covalent bond in the 90° TM–anion–TM bond angle, then the TM ion is ferromagnetic. As mentioned above, p–d coupling and hopping are strong in Fe- and Co-doped SnO$_2$. Therefore, in the close configuration, the local superexchange interaction between TM ions is ferromagnetic in Fe- and Co-doped SnO$_2$. Note that for the separated configuration, the superexchange will became weak. Moreover, in V- and Mn-doped SnO$_2$, because p–d coupling and hopping is weak, the superexchange is also weak and paramagnetism is the ground state for these doped systems. This does not necessarily exclude ferromagnetism from being induced by other kinds of mechanisms for all doped cases, such as F-center, double exchange, and carrier-mediated mechanisms. Concerning the magnetic properties, in table 1 we present the magnetic moments of the TM1 and TM2, which are ferromagnetically aligned. In the considered configurations, the magnetic moments of TM ions are almost independent of the TM distributions.

3.2. Oxygen vacancy effect

As mentioned above, TM–Vac(O)–TM groups are common in Fe-doped SnO$_2$ [2]. Therefore, even in pure SnO$_2$ as predicted by Kılıç and Zunger [35], Vac(O) has very low formation energy and would commonly exist. Thus, it is important to investigate the relations between TM ions and Vac(O) in the doped SnO$_2$. We choose the close configuration, in which the
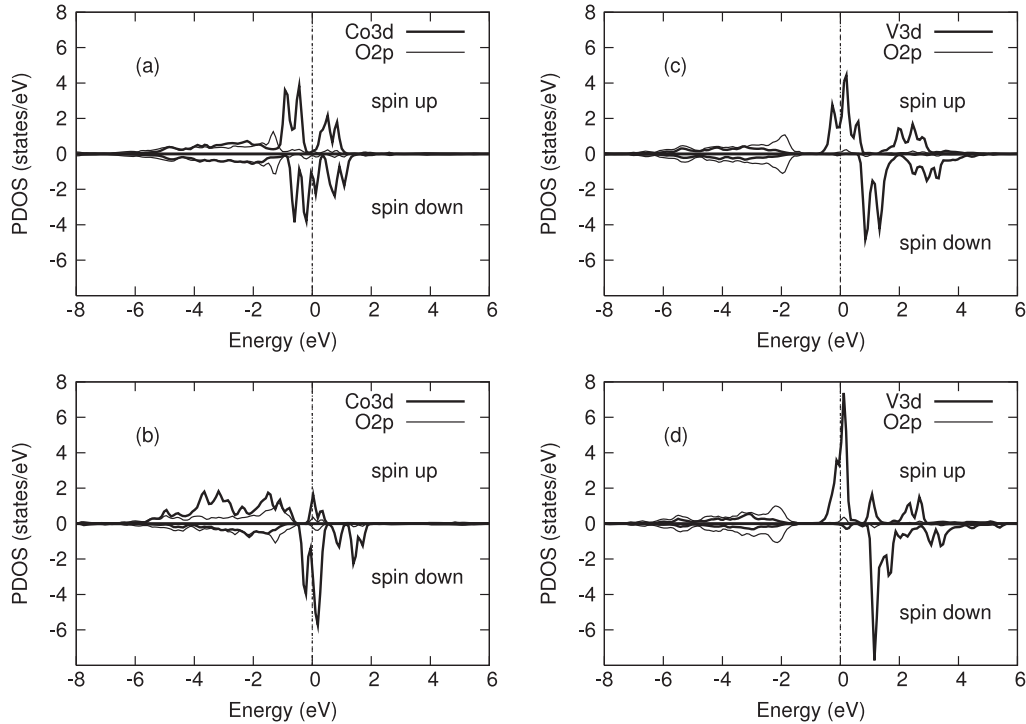
Figure 3. The partial density of states of TM ions 3d and O 2p with different distances between TM1 and oxygen vacancy (TM1–Vac(O)) of Co- and V-doped SnO_2 in the case of 12.5% doping. (a) The separation of Co–Vac(O) is 3.60 Å, (b) the separation of Co–Vac(O) is 2.06 Å, (c) the separation of V–Vac(O) is 3.60 Å, and (d) the separation of V–Vac(O) is 2.06 Å.

Table 2. The distances between oxygen vacancy (Vac(O)) and TM1, TM2 (in Å).

Composition	$Vac(O)_1$	$Vac(O)_2$	$Vac(O)_3$
TM1–Vac(O)	3.60	4.65	2.06
TM2–Vac(O)	4.24	2.06	2.06

TM ions are placed ferromagnetically. Relaxation around the vacancies is not performed. In terms of different distances between TM ions and Vac(O)s, as shown in table 2, we introduce three kinds of Vac(O)s named $Vac(O)_1$, $Vac(O)_2$, and $Vac(O)_3$ respectively. From $Vac(O)_1$ to $Vac(O)_3$, Vac(O) gradually moves closer to TM ions. The total energies of Vac(O)-contained systems are shown in table 3. These data show a strong tendency for Vac(O) to form close to Co and Fe ions, but V ions exclude Vac(O) strongly. Mn ions have a small influence on the distribution of Vac(O)s, and Vac(O)s tend to have an even distribution in Mn-doped SnO_2. Hence, TM–Vac(O)–TM groups will be abundant in Fe- and Co-doped SnO_2. In figures 3(a)–(d), we show the partial density of states (PDOS) of TM1 Co and V 3d as well as O 2p (TM1 and O ion located in the same octahedron) for two cases, in which the distances between TM1 and Vac(O) are 3.60 Å and 2.06 Å, respectively. When Vac(O) moves close to the TM1 (Co and V), the majority spins of Co 3d states, as shown in figures 3(a) and (b), are lower in energy and more strongly hybridized with the O 2p state, but the majority spin of the V 3d state, shown in figures 3(c) and (d), becomes more localized. Therefore, the total energies of the compounds decrease in Co-doped SnO_2 but increase in V-doped SnO_2 after the distances

between Vac(O) and TM ions decrease. This can be understood as follows. For charge balance, Fe and Co ions must have the ionic valence of Fe^{4+} and Co^{4+} in Fe- and Co-doped SnO_2 without introducing any defects. But Fe and Co ions do not have 4+ oxidation state, hence, in order to reach a more stable oxidation state, an adjacent Vac(O) is created for TM ions in Fe- and Co-doped SnO_2, and consequently Vac(O) has a strong attraction to Fe and Co ions. Conversely, V and Mn ions do have a 4+ oxidation state. As a result, they do not attract Vac(O) and even exclude it. Indeed, the localization of Vac(O) near the substitutional Co ion has been reported in Co-doped TiO_2 both theoretically and experimentally [18, 36].

Regarding the magnetic properties of the Vac(O)-contained systems, in table 4 we present magnetic moments of the TM1 and TM2 as well as the total moments of the supercells in the presence of three kinds of Vac(O)s. These data show that the presence of Vac(O) increases the magnetic moments of the TM ions as well as the supercells in all doping cases except for the Co-doped $Vac(O)_1$-contained system. One can also find that the magnetic moments of TM ions and supercells increase with Vac(O) moving close to TM ions. Moreover, there exists a sharp increase in the magnetic moments when TM ions and Vac(O) are located in the same octahedron, in which the distance between TM ion and Vac(O) is 2.06 Å. All these results show that Vac(O) has a strong influence on the magnetic properties of TM ion-doped SnO_2, especially for Fe and Co-doped cases, since Fe and Co ions have a strong attraction with Vac(O). Hence, it could be understood that the magnetic properties strongly depend on the different experimental methods and conditions.

Table 3. Total energies of the supercells for three kinds of Vac(O)s-contained systems (in eV).

System	Fe-doped SnO_2	Co-doped SnO_2	Mn-doped SnO_2	V-doped SnO_2
Vac(O)$_1$	−44 992.889	−45 223.428	−44 504.093	−43 996.002
Vac(O)$_2$	−44 993.364	−45 223.678	−44 504.082	−43 995.263
Vac(O)$_3$	−44 994.029	−45 224.021	−44 504.222	−43 994.553

Table 4. Magnetic moments (in μ_B) of the TM1 (μ^{TM1}), TM2 (μ^{TM2}) and the supercell total moments (μ^{SC}) in the presence of three kinds of Vac(O)s (Vac(O)$_1$, Vac(O)$_2$, and Vac(O)$_3$).

System	V-doped SnO_2 $\mu^{TM1}/\mu^{TM2}/\mu^{SC}$	Mn-doped SnO_2 $\mu^{TM1}/\mu^{TM2}/\mu^{SC}$	Fe-doped SnO_2 $\mu^{TM1}/\mu^{TM2}/\mu^{SC}$	Co-doped SnO_2 $\mu^{TM1}/\mu^{TM2}/\mu^{SC}$
Vac(O)$_1$	1.22/1.29/2.00	3.25/3.27/6.15	3.88/3.87/9.02	0.49/0.52/1.36
Vac(O)$_2$	1.28/1.77/3.01	3.29/3.82/7.11	3.89/4.05/9.41	0.83/2.50/4.20
Vac(O)$_3$	1.63/1.80/3.55	3.84/3.85/7.93	4.05/4.07/9.93	2.33/2.83/6.94
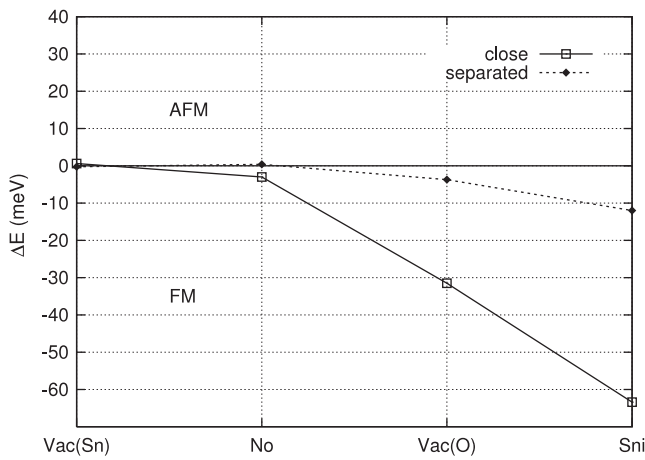
Figure 4. The energy difference ΔE between FM and AFM of V-doped SnO_2 with a doping concentration of 12.5% in the presence of defects and additional carriers for the separated and close configurations.

3.3. V-doped SnO_2 with additional carriers

As presented in figure 2, based on the above calculations about V-doped SnO_2 without introducing any defects and additional carriers, it is found that doping SnO_2 with V is not a good choice to obtain high Curie temperature FM in doped SnO_2. However, in diluted magnetic semiconductors such as Mn-doped GaAs, additional carriers play a key role in the FM behavior of this system. As mentioned above, experimentally the magnetic properties of V-doped ZnO [20] with high Curie temperature depend on the doping concentration and the density of n-type carriers. Therefore, we further investigate V-doped SnO_2 systems with defects and additional carriers being introduced. We simulate the n-type doping by introducing Vac(O) and tin interstitial (Sni), and the p-type doping by tin vacancy (Vac(Sn)). These defects are located as far as possible from V ions. The obtained energy difference ΔE in the presence of three kinds of defects is shown in figure 4. For comparison, former results about V-doped SnO_2 without any additional carriers are again plotted (labeled as No) in figure 4.

The ground state of this compound stays as paramagnetism even after introducing p-type doping (Vac(Sn)). But

ΔE becomes negative after introducing n-type doping (Vac(O) and Sni), accordingly n-type doping strongly stabilizes the ferromagnetic state. This result clearly shows the difference between doped SnO_2 and doped ZnO, for that Spaldin has claimed that FM is not obtained in Co- and Mn-doped ZnO unless additional p-type carriers are introduced [15]. It can also be observed from figure 4 that ΔE s of Sni doping are twice as large as that of Vac(O) doping in both separated and close configurations. Note that, Vac(O) and Sni provide two and four electrons in the supercells, respectively. Hence, the Curie temperature of the compound is directly related to the density of n-type carriers. In the n-type doping cases, the absolute values of ΔE rapidly increase when V ions move close to each other. For example, in the case of Sni doping, ΔE in the close configuration is about five times as large as that of the separated configuration. Therefore, the ferromagnetic state becomes more stable with the concentration of V ions increasing. A simple term for n-doping causing an increase in FM coupling in V-doped SnO_2 can be derived from the density of states behavior. As shown in figure 5(a), just from the rigid band point of view, the n-type doping will shift the Fermi level to the valley leading to the enhancement of the magnetism. This results in the increase of FM coupling in V-doped SnO_2.

The above results show that spin flipping energy (and thus the Curie temperature) of V-doped SnO_2 increases with the concentration of V ions as well as the density of n-type carriers. As a result, there are two possible ways to realize high Curie temperatures in V-doped SnO_2. One is to increase the doping concentration of V ions, and the other is to raise the density of n-type carriers. Looking through the PDOS of TM ions (V and Co) 3d and O 2p in the case where the TM ions and O ion locate in the same octahedron, as shown in figures 5(a) and (b) for 6.5% doping concentration, the hybridization between V 3d and O 2p is small compared with the hybridization between Co 3d and O 2p. Therefore, only a smaller doping concentration of V-doped SnO_2 than that of Co-doped SnO_2 may be achieved. This leads to the fact that it is difficult to realize high doping concentration in V-doped SnO_2. Nevertheless, since rutile SnO_2 has n-type conduction [35], a larger density of n-type carriers can be generated in rutile SnO_2 by additional doping. Hence, raising the density of n-type carriers might be a practical way to realize
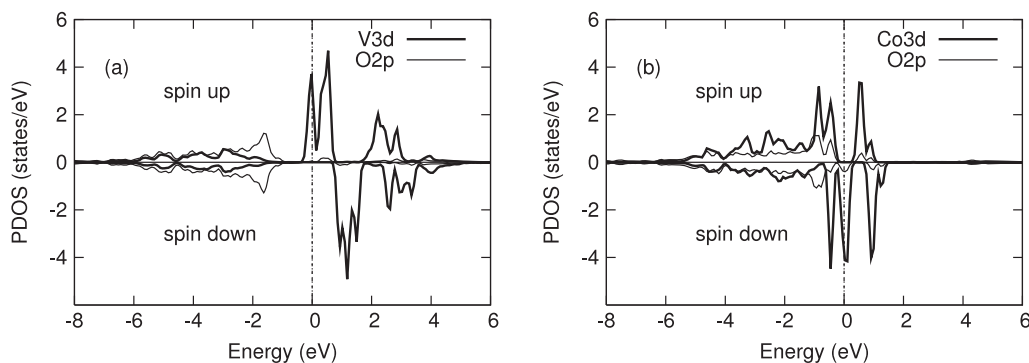
Figure 5. The partial density of states of TM1 3d and O 2p of V- and Co-doped SnO_2 with the doping concentration 6.5%. (a) for V-doped SnO_2, (b) for Co-doped SnO_2.

high Curie temperatures in V-doped SnO_2, for example by using Sb doping, about which we still expect to have more experimental evidence.

4. Summary

In conclusion, we have investigated the electronic structures of TM ion (V, Mn, Fe, and Co)-doped SnO_2. Our calculations show that ferromagnetism is obtained by doping SnO_2 with Fe and Co ions and paramagnetism is the ground state in V- and Mn-doped SnO_2. Oxygen vacancy has a strong influence on the magnetic properties of these TM ion-doped compounds. There is a strong tendency for an oxygen vacancy to form complexes with Co and Fe ions, indicating that TM–oxygen vacancy–TM groups will be common in Fe- and Co-doped SnO_2, but are not easily formed in V- and Mn-doped SnO_2. Additional n-type carriers are required to stabilize the ferromagnetic state and the Curie temperature increases with increasing densities of n-type carriers in V-doped SnO_2. We also propose that raising the density of n-type carriers is a possible practical way to obtain high Curie temperatures in V-doped SnO_2.

Acknowledgments

References

[1] Ogale S B, Choudhary R J, Buban J P, Lofland S E, Shinde S R, Kale S N, Kulkarni V N, Higgins J, Lanci C, Simpson J R, Browning N D, Das Sarma S, Drew H D, Greene R L and Venkatesan T 2003 *Phys. Rev. Lett.* **91** 077205
[2] Coey J M D, Douvails A P, Fitzgerald C B and Venkatesan M 2004 *Appl. Phys. Lett.* **84** 1332
[3] Matsumoto Y, Murakami M, Shono T, Hasegawa T, Fukumura T, Kawasaki M, Ahmet P, Chikyou T, Koshihara S and Koinuma H 2001 *Science* **291** 854
[4] Ueda K, Tabata H and Kawai T 2001 *Appl. Phys. Lett.* **79** 988
[5] Ramachandran S, Tiwari Ashutosh and Narayan J 2004 *Appl. Phys. Lett.* **84** 5255
[6] Venkatesan M, Fitzgerald C B, Lunney J G and Coey J M D 2004 *Phys. Rev. Lett.* **93** 177206
[7] HoaHong N, Sakai J, Prellier W, Hassini A, Ruyter A and Gervais F 2004 *Phys. Rev.* B **70** 195204
[8] Hong N H, Sakai J, Huong N T, Poirot N and Ruyter A 2005 *Phys. Rev.* B **72** 045336
[9] Punnoose A, Hays J, Thurber A, Engelhard M H, Kukkadapu R K, Wang C, Shutthanandan V and Thevuthasan S 2005 *Phys. Rev.* B **72** 054402
[10] Hays J, Punnoose A, Baldner R, Engelhard M H, Peloquin J and Reddy K M 2005 *Phys. Rev.* B **72** 075203
[11] Janisch R and Spaldin N A 2006 *Phys. Rev.* B **73** 035201
[12] Shinde S R, Ogale S B, Higgins J S, Zheng H, Millis A J, Kulkarni V N, Ramesh R, Greene R L and Venkatesan T 2004 *Phys. Rev. Lett.* **92** 166601
[13] Sato K and Katayama-Yoshida H 2000 *Japan. J. Appl. Phys.* 2 **39** L555
[14] Park M S, Kwon S K and Min B I 2002 *Phys. Rev.* B **65** 161201(R)
[15] Spaldin N A 2004 *Phys. Rev.* B **69** 125201
[16] Park M S and Min B I 2003 *Phys. Rev.* B **68** 224436
[17] Wang Q, Sun Q, Rao B K and Jena P 2004 *Phys. Rev.* B **69** 233310
[18] Jaffe J E, Droubay T C and Chambers S A 2005 *J. Appl. Phys.* **97** 073908
[19] Errico L A, Rentería M and Weissmann M 2005 *Phys. Rev.* B **72** 184425
[20] Saeki H, Tabata H and Kawai T 2001 *Solid State Commun.* **120** 439
[21] Hohenherg P and Kohn W 1964 *Phys. Rev.* **136** B864
[22] Soler J M, Artacho E, Gale J D, García A, Junquera J, Ordejón P and Sánchez-Portal D 2002 *J. Phys.: Condens. Matter* **14** 2745
[23] Sánchez-Portal D, Ordejón P, Artacho E and Soler J M 1997 *Int. J. Quantum Chem.* **65** 453 and references therein
[24] Ordejón P 2000 *Phys. Status Solidi* b **217** 335
[25] Troullier N and Martins J L 1991 *Phys. Rev.* B **43** 1993
[26] Louie S G, Froyen S and Cohen M L 1982 *Phys. Rev.* B **26** 1738
[27] Postnikov A V, Entel P and Ordejón P 2002 *Phase Transit.* **75** 143
[28] Robles R, Izquierdo J, Vega A and Balbás L C 2001 *Phys. Rev.* B **63** 172406
[29] Sánchez-Portal D, Martin R M, Kauzlarich S M and Pickett W E 2002 *Phys. Rev.* B **65** 144414

[30] Izquierdo J, Vega A, Balbás L C, Sánchez-Portal D, Junquera J, Artacho E, Soler J M and Ordejón P 2000 *Phys. Rev.* B **61** 13639

[31] Perdew J P, Burke K and Ernzerhof M 1996 *Phys. Rev. Lett.* **77** 3865

[32] Ceperley D M and Alder B J 1980 *Phys. Rev. Lett.* **45** 566

[33] Monkhorst H J and Pack J D 1976 *Phys. Rev.* B **13** 5188

[34] Kimura H, Fukumura T, Kawasaki M, Lnaba K, Hasegawa T and Koinuma H 2002 *Appl. Phys. Lett.* **80** 94

[35] Kılıç Çetin and Zunger Alex 2002 *Phys. Rev. Lett.* **88** 095501

[36] Chambers S A, Heald C M and Droubay T 2005 *Phys. Rev.* B **67** 100401(R)